


Experimental Verification of Multicopy Activation of Genuine Multipartite EntanglementRobert Stárek^{1,*}, Tim Gollerthan², Olga Leskovjanová¹, Michael Meth², Peter Tirlir², Nicolai Friis³,
Martin Ringbauer², and Ladislav Mišta, Jr.^{1,†}¹*Department of Optics, Palacký University, 17. listopadu 1192/12, 779 00 Olomouc, Czech Republic*²*Universität Innsbruck, Institut für Experimentalphysik, 6020 Innsbruck, Austria*³*Technische Universität Wien, Atominstytut and Vienna Center for Quantum Science and Technology (VCQ),
Stadionallee 2, 1020 Vienna, Austria* (Received 21 October 2025; accepted 27 February 2026; published 20 April 2026)

A central concept in quantum information processing is genuine multipartite entanglement (GME), a type of correlation beyond biseparability, that is, correlations that cannot be explained by statistical mixtures of partially separable states. GME is relevant for characterizing and benchmarking complex quantum systems, and it is an important resource for applications such as quantum communication. Remarkably, it has been found that GME can be activated from multiple copies of biseparable quantum states, which do not possess GME individually. Here, we experimentally demonstrate unambiguous evidence of such GME activation from two copies of a biseparable three-qubit state in a trapped-ion quantum processor. These results not only challenge notions of quantum resources but also highlight the potential of using multiple copies of quantum states to achieve tasks beyond the capabilities of the individual copies.

DOI: [10.1103/kv4s-tfc6](https://doi.org/10.1103/kv4s-tfc6)

A key goal in the development of quantum-communication technology is to establish large-scale quantum networks [1–5]. Central questions in this endeavor pertain to understanding what kind of quantum states can be established by specific networks [6–9], which resources are required to do so, and how the successful generation can be efficiently verified [10–12]. A particular focus of these efforts (on the side of both theory, see, e.g., Refs. [13–15], and experiments, see, e.g., Refs. [16–20]) is the generation of *genuinely multipartite entangled* states, needed to harness the full potential of quantum networks. Such states are not just fully inseparable in the sense that they are entangled across all bipartitions, but they also cannot be decomposed into statistical mixtures of states that are separable with respect to different partitions, whereas all states that admit such decompositions are called biseparable. For an introduction, we refer to Ref. [21] [Chapter 18]. Multipartite entanglement is considered to be an important resource for tasks in quantum metrology [22], quantum computing (e.g., for measurement-based quantum computation [23,24] and quantum error correction

[25]), and quantum communication (e.g., for quantum key distribution [26,27], conference key agreement [28], or communication problems in networks [29]), and there are some applications for which genuine multipartite entanglement (GME) specifically is crucial [26,30].

Remarkably, it has been shown that considering more than one copy of a state drastically changes the distinction between full inseparability and GME [31,32]: where one copy of a state may be biseparable, two or more copies can be GME as long as the single-copy state is fully inseparable (i.e., entangled with respect to all bipartitions)—a phenomenon dubbed *activation of GME*. Moreover, it was shown that every fully inseparable biseparable state can be activated for some number of copies [33], even in infinite dimensions [34].

A pressing question that follows on the heel of these observations is *How difficult is it to harness the activation of GME?* Theoretical work in this direction [35] has already demonstrated that there are some fully inseparable biseparable states whose activated GME cannot be projected back to the single-copy level. In addition, some cases might require prohibitively many copies for activation, and some states with activated GME might require joint local operations on multiple copies that are difficult to realize in practice in order to verify or use the activated multipartite correlations.

Here, we make crucial steps toward bringing the utilization of GME activation closer to practical reality by unambiguously demonstrating its core principle. We experimentally prepare two copies of a biseparable three-qubit

*Contact author: starek@optics.upol.cz†Contact author: mista@optics.upol.cz

state on two groups of three trapped ions and show that the two-copy state is genuinely multipartite entangled. Whereas previous work in this direction [36] only checked necessary (but not sufficient) conditions for biseparability of the individual copies, state preparation in our experiment solely employs operations that cannot produce genuinely multipartite entangled three-qubit states or bipartite entanglement between the two single-copy instances of the three-qubit states. In addition, explicit biseparable decompositions for the initial three-qubit states are determined by a numerical algorithm [37,38]. We confirm the activation of GME by employing a suitable GME witness for the two-copy state. Our results thus provide clear evidence of two-copy GME activation. This marks a significant step in the exploration of quantum resources that can be harnessed by jointly but locally accessing multiple copies of distributed quantum states in the laboratory.

Theory—In order to experimentally demonstrate multi-copy GME activation, we consider a state ρ_{ABC} of three qubits that is biseparable, i.e., can be written as a statistical mixture of states $\rho_{A|BC}$, $\rho_{AB|C}$, and $\rho_{B|AC}$ that are separable with respect to the bipartitions $A|BC$, $AB|C$, and $B|AC$, respectively, but which is fully inseparable, that is, ρ_{ABC} cannot be written as a statistical mixture of terms that are all separable with respect to any fixed bipartition. Yet, ρ_{ABC} is two-copy activatable: two copies $\rho_{A_1B_1C_1} \otimes \rho_{A_2B_2C_2}$ of this state are GME, i.e., the joint two-copy state is not biseparable with respect to the partition $A_1A_2|B_1B_2|C_1C_2$. In addition, we are interested in a state that is sufficiently robust with respect to these properties: small perturbations should not change the biseparability and full inseparability of the single copy or the GME of two copies. We are also interested in an implementation that is closest to the original spirit of activation, namely that each copy is prepared directly as a convex mixture of product states without using any operation that could potentially generate GME. However, the potentially large number of states in such mixtures, combined with the need to prepare multiple copies, might lead to significant overhead in terms of the number of required reconfigurations of the experimental setup. To keep this number at a level achievable with current technology, we construct an activatable state in which the number of components is sufficiently small.

By combining analytical and numerical calculations, we arrived at a suitable candidate for the desired state in the form of the balanced mixture,

$$\tilde{\rho}_{ABC} = \frac{1}{8} \sum_{i=0}^7 |a_i\rangle\langle a_i|, \quad (1)$$

of only eight three-qubit states $|a_i\rangle$, $i = 0, 1, \dots, 7$. The first four of these have the form

$$|a_{0,1}\rangle = |\pm\rangle_A \otimes |\Phi^\pm\rangle_{BC}, \quad (2a)$$

$$|a_{2,3}\rangle = (\sqrt{Z} \otimes \sqrt{Z} \otimes Z)|\pm\rangle_A \otimes |\Phi^\pm\rangle_{BC}, \quad (2b)$$

while the remaining four, $|a_{4,\dots,7}\rangle$, arise from them by swapping qubits A and B . Here, the subscripts 0 and 2, and 1 and 3 on the left side refer to the signs $+$ and $-$ on the right side, $|\Phi^\pm\rangle = (|00\rangle \pm |11\rangle)/\sqrt{2}$, $|\pm\rangle = (|0\rangle \pm |1\rangle)/\sqrt{2}$, Z is the Pauli- z matrix, and $\sqrt{Z} = \text{diag}(1, i)$.

The state $\tilde{\rho}_{ABC}$ defined in Eq. (1) is clearly a convex mixture of separable states with respect to the partitions $A|BC$ and $B|AC$ and is thus biseparable by construction as required. This state is also fully inseparable and therefore meets the criteria for being activatable [33]. In addition, its two copies, $\tilde{\rho}_{A_1B_1C_1} \otimes \tilde{\rho}_{A_2B_2C_2}$, are GME across the partition $A_1A_2|B_1B_2|C_1C_2$, as shown below, and the state is thus also two-copy GME activatable. This is somewhat surprising when we realize that we only need a *single* two-qubit CNOT operation to prepare each constituent of the state $\tilde{\rho}_{ABC}$, which obviously cannot generate GME. Experimental activation of GME based on the state $\tilde{\rho}_{ABC}$ [Eq. (1)] would thus represent a practically ideal demonstration of this counterintuitive effect of obtaining “something from nothing.” But before we move on to that, let us first prove GME in two copies of this state.

The GME can be shown by finding a witness with respect to the partition $A_1A_2|B_1B_2|C_1C_2$ for its two-copy state which we for convenience rearrange as $\tilde{\rho}_{A_1A_2B_1B_2C_1C_2}$. In general, a GME witness is a Hermitian operator W for which $\text{Tr}[W\rho^{\text{bisep}}] \geq 0$ for all biseparable states ρ^{bisep} and $\text{Tr}[W\rho] < 0$ for at least one GME state ρ . The GME of a number of states, including two copies of the state $\tilde{\rho}_{ABC}$ [Eq. (1)], can be detected using so-called *fully decomposable witnesses*, which can be written as [39]

$$W = P_M + Q_M^{T_M}, \quad (3)$$

for every subset M of all systems. Here, P_M and Q_M are positive semidefinite matrices and the superscript T_M denotes the partial transposition with respect to part M of the whole system [40,41]. The important upside of a fully decomposable witness is that it can be found relatively simply by solving a semidefinite program (SDP) [39]. In our case, the SDP is

$$\begin{aligned} & \underset{W, P_k}{\text{minimize}} \text{Tr}[W\tilde{\rho}_{A_1A_2B_1B_2C_1C_2}] \\ & \text{subject to } \text{Tr}[W] = 1, \\ & P_k \geq 0, \\ & Q_k = (W - P_k)^{T_k} \geq 0, \\ & \text{for } k = \{A_1A_2, B_1B_2, C_1C_2\}. \end{aligned} \quad (4)$$

We solve this SDP numerically and obtain $\text{Tr}[W\tilde{\rho}_{A_1A_2B_1B_2C_1C_2}] = -1.042 \times 10^{-2}$, verifying that the

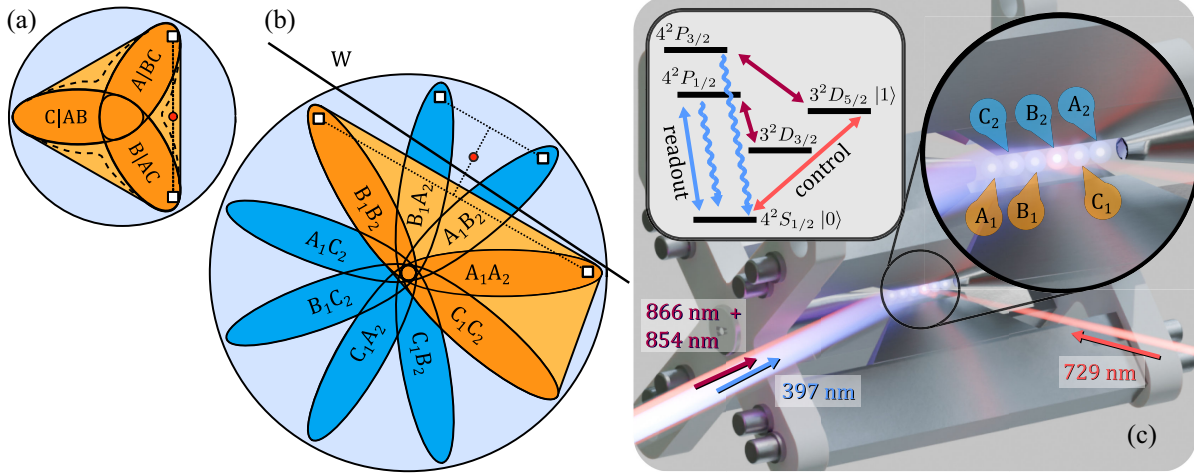


FIG. 1. (a) Illustration of the robust biseparable two-copy GME-activatable state ρ_{ABC} [Eq. (6)]. The dark orange oval regions represent the sets of separable states across bipartitions $A|BC$, $B|AC$, and $C|AB$. The light orange regions represent the GME-activatable states. The union of the orange regions represents the set of biseparable states, and the light blue region outside contains the GME states. The orange regions between the dashed lines and the borders between the sets of biseparable and GME states represent the set of biseparable two-copy GME-activatable states. The state ρ_{ABC} (red dot) is a balanced mixture (illustrated by the dotted line) of states separable across bipartitions $A|BC$ and $B|AC$ (white squares), respectively. (b) Diagrammatic representation of two copies of the state ρ_{ABC} . The oval regions labeled by jk with $j = A_1, B_1, C_1$ and $k = A_2, B_2, C_2$ denote sets of states for which the pair of qubits j and k is separable from the rest of the system. The convex hull of the three oval orange regions indicates the set of biseparable states with respect to the partition $A_1A_2|B_1B_2|C_1C_2$. The two-copy state $\rho_{A_1A_2B_1B_2C_1C_2}$ (red dot) is a balanced mixture (illustrated by the dotted lines) of four possible tensor products of states depicted by white squares in panel (a), which belong to the sets A_1A_2 , B_1B_2 , A_1B_2 , and B_1A_2 (white squares), respectively. GME with respect to the partition $A_1A_2|B_1B_2|C_1C_2$ is detected by the witness W (solid black line). (c) Illustration of a linear Paul trap and a $^{40}\text{Ca}^+$ level diagram. A Paul trap consisting of four blade electrodes and two tip electrodes confines a linear chain of six $^{40}\text{Ca}^+$ ions (white dots). The orange and blue labels illustrate the interleaved qubit assignment of the first and second copies. We refer to the main text for details on the energy-level diagram.

witness faithfully detects GME of two copies of the state $\tilde{\rho}_{ABC}$ as desired. The witness W has nonzero matrix elements only on the main diagonal and antidiagonal, with elements $1/12$ that are listed explicitly together with the matrices P_M and Q_M in Supplemental Material Sec. I [42]. Additionally, W can be decomposed into a sum of 32 six-qubit Pauli strings M_k ,

$$W = \sum_{k=0}^{31} m_k M_k, \quad (5)$$

with weights m_k (see Supplemental Material Sec. I [42] for the list of these products and their weights). Half of the matrices M_k correspond to computational basis measurements of various subsets and can thus be measured at once. Hence, this decomposition is experimentally very convenient and allows for a direct witness measurement using only 17 distinct measurement settings. This is much less expensive than the $3^6 = 729$ settings required for Pauli state tomography.

The state in Eq. (1) lies close to the boundary of the set of biseparable states, and the biseparability condition is thus highly sensitive to experimental errors. This obstacle can be circumvented by admixing a small fraction $q = 6 \times 10^{-2}$ of

colored noise in the form of $(|\tilde{a}_8\rangle\langle\tilde{a}_8| + |\tilde{a}_9\rangle\langle\tilde{a}_9|)/2$ with $|\tilde{a}_8\rangle = |001\rangle_{ABC}$ and $|\tilde{a}_9\rangle = |110\rangle_{ABC}$ to the state in Eq. (1). The exact value of $q = 6 \times 10^{-2}$ was selected based on the preliminary analysis of the single-copy states in our experiment, as is explained in more detail in Supplemental Material Sec. II [42].

This gives

$$\rho_{ABC} = \frac{1-q}{8} \sum_{i=0}^7 |a_i\rangle\langle a_i| + \frac{q}{2} (|\tilde{a}_8\rangle\langle\tilde{a}_8| + |\tilde{a}_9\rangle\langle\tilde{a}_9|). \quad (6)$$

The obtained state is simple, manifestly biseparable, and experimentally robust [see Fig. 1(a) for a pictorial representation]. For the GME witness W one further expects $\langle W \rangle = \text{Tr}[W\rho_{A_1A_2B_1B_2C_1C_2}] = -0.887 \times 10^{-2}$, which certifies two-copy GME activatability of the state, as illustrated in Fig. 1(b).

Experimental GME activation—We prepared two copies of the state in Eq. (6) on a trapped-ion quantum processor [43]. It employs a linear Paul trap, where six $^{40}\text{Ca}^+$ ions—three for each copy—were confined [see Fig. 1(c)]. Qubits are encoded in the electronic states $|0\rangle = 4^2S_{1/2}(m_j = -1/2)$ and $|1\rangle = 3^2D_{5/2}(m_j = -1/2)$ and are coherently controlled via a narrow band laser driving an electric

quadrupole transition at 729 nm. As illustrated in Fig. 1(c), the short-lived $4^2P_{1/2}$ state and the $4^2S_{1/2}$ state are coupled via a 397 nm laser, which allows for the effective implementation of both Doppler and polarization-gradient cooling. Ions spontaneously decaying to the $3^2D_{3/2}$ level are pumped back into the cooling cycle with a 866 nm laser. Furthermore, another laser at 854 nm permits population transfer from $3^2D_{5/2}$ to the short-lived $4^2P_{3/2}$ state, which decays back to $4^2S_{1/2}$. This closed cycle enables cooling to the motional ground state via resolved sideband cooling.

State preparation control sequences include individually addressed qubit rotations around arbitrary axes in the equatorial plane of the Bloch sphere, virtual Z gates, and entangling Mølmer–Sørensen gates applied to arbitrary pairs of qubits [44]. The latter were used to generate the Bell states $|\Phi^\pm\rangle$ in Eq. (2) from the ground state $|00\rangle$. The two copies of the three-qubit states in Eq. (6) were prepared on ions 0, 2, and 4 as well as on ions 5, 3, and 1, respectively, with ions indexed according to their positioning in the trap. This ordering is chosen to reduce imperfections in the addressing of neighboring ions. The \sqrt{Z} gates of Eq. (2) and swap gates were implemented virtually—the former by adjusting the phase of consecutive pulses, the latter by relabeling the ions. Projective measurements are performed at the end of the gate sequence by driving the $4^2S_{1/2}$ to $4^2P_{1/2}$ transition with a 397 nm laser and collecting the fluorescence. Ions in the states $|0\rangle$ and $|1\rangle$ are discriminated by their respective bright or dark appearance with a readout error below 2×10^{-3} .

To verify the quality of the prepared single copies and assess their biseparability, we opted for quantum-state tomography. Moreover, the single-copy density matrices are later used to predict the mean value of the witness, which certifies GME activation from three copies. We performed tomographic characterization separately for each of the ten prepared three-qubit states, $|a_i\rangle$, $i = 0, \dots, 7$, and $|\tilde{a}_j\rangle$, $j = 8, 9$, using Pauli tomography with 200 shots per measurement configuration and constituent state. The constituent state density matrices were then individually reconstructed via a maximum-likelihood estimation algorithm [45] and subsequently incoherently mixed as in Eq. (6) with the mixing factor of $q = 6 \times 10^{-2}$. Uncertainties were calculated using 100 runs of Monte Carlo resampling. From these tomographies, we extract infidelities $1 - F$ of the two single-copy states with the target state in Eq. (6) of $(2.54 \pm 0.05) \times 10^{-2}$ and $(1.30 \pm 0.06) \times 10^{-2}$, respectively.

Next, we certified the biseparability of the single copies. For this purpose, we used the numerical algorithm of Refs. [37,38], based on the sequential subtraction of product states from the investigated density matrix, which is described in detail in Supplemental Material Sec. II [42]. The algorithm effectively decomposes the original density matrix into a sum of product states and a small fully separable remainder, thereby proving its biseparability.

Because of the structure of state ρ_{ABC} defined in Eq. (6), we had to modify the algorithm. This is because reducing the contributions from any of the $|a_i\rangle\langle a_i|$ or $|\tilde{a}_i\rangle\langle \tilde{a}_i|$ to the original state ρ_{ABC} would actually *increase* the purity, which would be in contradiction to the requirements of the original algorithm. The key modification is to subtract a biseparable mixture instead, which is described in detail in Supplemental Material Sec. II [42]. We applied the modified algorithm to each of the sampled matrices, as well as to the original reconstruction. The algorithm converged for both single-copy original density matrices and in 95% and 99% of their Monte Carlo samples, respectively. In the remaining cases, we must report an inconclusive result.

Finally, GME activation was observed experimentally. To measure the mean value of the witness, $\langle W \rangle$, we sequentially prepared all possible products $|\psi\rangle \otimes |\phi\rangle$ with $|\psi\rangle, |\phi\rangle \in \{|a_i\rangle_{i=0,\dots,7}\} \cup \{|\tilde{a}_8\rangle, |\tilde{a}_9\rangle\}$, where the first tensor factor refers to qubits $A_1B_1C_1$ and the second to qubits $A_2B_2C_2$.

The state $\rho_{A_1B_1C_1} \otimes \rho_{A_2B_2C_2}$ was converted into $\rho_{A_1A_2B_1B_2C_1C_2}$ using swap gates. For each of the 10×10 constituents of that state, we then performed the Pauli measurements M_k appearing in the decomposition described by Eq. (5) with 50 shots each. The first 16 terms M_k , $k = 0, 1, \dots, 15$, were measured at once by measuring all qubits in the Z basis. From the measured data, we then calculated the witness mean and its statistical error using the vector formalism described in Supplemental Material Sec. III [42]. The estimated witness mean value is

$$\langle W \rangle = (-5.7 \pm 0.5) \times 10^{-3}, \quad (7)$$

which is more than eleven standard deviations below zero. This convincingly verifies the presence of GME in the two-copy state and completes our experimental demonstrations of multicopy GME activation.

Discussion and conclusion—We have experimentally verified two-copy GME activation with state-of-the-art trapped-ion qubits. Our results thereby represent a crucial first step toward the exploration and utilization of quantum resources that are unlocked by jointly processing locally accessible subsystems of multiple copies. At the same time, our results highlight the challenges that will arise in attempts to harness higher levels of the GME activation hierarchy [32]: one lies in the exponential growth of the number of constituents of the considered multicopy mixed states. While our two-copy experiment required the preparation of 100 combinations, a straightforward extension to three copies would require 1000. Another factor is the significant increase in resource requirements for witness-based GME certification and biseparability checks. For instance, for three-copy GME activation of the mixture given by Eq. (6) with $q = 0.26$, the SDP defined in Eq. (4)

does not find any two-copy GME witness. However, a three-copy witness comprising 128 Pauli strings exists; its evaluation requires four times more measurements compared to the two-copy witness tested here. To verify two-copy biseparability of the experimentally prepared states via the subtraction algorithm would also require demanding six-qubit quantum tomography on each copy pair.

The above obstacles are all technical in nature and can be overcome by finding simpler three-copy GME activatable states and/or streamlining the process of preparing and measuring the states used. As three-copy GME activation is a more subtle effect, the tolerance to infidelities becomes narrower. To assess its feasibility, one should also take into account the effect on the measurement uncertainty. Therefore, we used the available reconstruction of the two realizations of single copies and extrapolated the density matrix of the three-copy state in silico for the case $q = 0.26$. The fidelity of this density matrix to the ideal theoretical state would be 0.954, leading to an expected witness value of $\langle W \rangle = (-7 \pm 4) \times 10^{-5}$ when using 50 shots per setting. Compared to the theoretical value for a perfect state of $\langle W \rangle = -8.5 \times 10^{-4}$, this indicates that observing three-copy GME activation is quite time consuming, yet achievable.

Having demonstrated the feasibility of accessing GME from two copies of biseparable states, an exciting next step will be to observe and utilize GME activation on spatially separated systems in a multiparty quantum network. The states used in our demonstration are indeed typical for what one might expect in a quantum network with bipartite entanglement sources.

Acknowledgments—We acknowledge support from the Austrian Science Fund (FWF) through Project No. P36478-N funded by the European Union—NextGenerationEU and through the EU-QUANTERA Project No. TNiSQ (N-6001), as well as from the Austrian Federal Ministry of Education, Science and Research via the Austrian Research Promotion Agency (FFG) through the flagship project HPQC Projects No. FO999897481 and No. FO999914030 (MUSIQ), and No. FO999921407 (HDcode) funded by the European Union—NextGenerationEU. O.L. acknowledges support from Palacký University, under Grant No. IGA-PrF-2025-010. R.S. acknowledges support from the Ministry of the Interior of the Czech Republic through NU-CRYPT Project No. VK01030193 and from the Ministry of Education, Youth and Sports of the Czech Republic under Grant No. 8C22003 (QD-E-QKD) of the QuantERA II Programme that has received funding from the European Union’s Horizon 2020 research and innovation programme under Grant Agreement No. 101017733. We thank Jan Provazník for building and maintaining the

computational cluster at Palacký University, Department of Optics.

Data availability—The data that support the findings of this article are openly available [46].

- [1] H. J. Kimble, *Nature (London)* **453**, 1023 (2008).
- [2] W. Dür, R. Lamprecht, and S. Heusler, *Eur. J. Phys.* **38**, 043001 (2017).
- [3] C. Simon, *Nat. Photonics* **11**, 678 (2017).
- [4] S. Wehner, D. Elkouss, and R. Hanson, *Science* **362**, eaam9288 (2018).
- [5] A. S. Cacciapuoti, M. Caleffi, F. Tafuri, F. S. Cataliotti, S. Gherardini, and G. Bianchi, *IEEE Network* **34**, 137 (2020).
- [6] M. Navascués, E. Wolfe, D. Rosset, and A. Pozas-Kerstjens, *Phys. Rev. Lett.* **125**, 240505 (2020).
- [7] M. Navascués and E. Wolfe, *J. Causal Infer.* **8**, 70 (2020).
- [8] T. Kraft, S. Designolle, C. Ritz, N. Brunner, O. Gühne, and M. Huber, *Phys. Rev. A* **103**, L060401 (2021).
- [9] E. Wolfe, A. Pozas-Kerstjens, M. Grinberg, D. Rosset, A. Acín, and M. Navascués, *Phys. Rev. X* **11**, 021043 (2021).
- [10] T. Kraft, C. Spee, X.-D. Yu, and O. Gühne, *Phys. Rev. A* **103**, 052405 (2021).
- [11] K. Hansenne, Z.-P. Xu, T. Kraft, and O. Gühne, *Nat. Commun.* **13**, 496 (2022).
- [12] N. K. H. Li, X. Dai, M. H. Muñoz-Arias, K. Reuer, M. Huber, and N. Friis, *Nat. Commun.* **17**, 1707 (2026).
- [13] P. Contreras-Tejada, C. Palazuelos, and J. I. de Vicente, *Phys. Rev. Lett.* **126**, 040501 (2021).
- [14] P. Contreras-Tejada, C. Palazuelos, and J. I. de Vicente, *Phys. Rev. Lett.* **128**, 220501 (2022).
- [15] S. Morelli, D. Sauerwein, M. Skotiniotis, and N. Friis, *Quantum* **6**, 722 (2022).
- [16] J.-C. Besse, K. Reuer, M. C. Collodo, A. Wulff, L. Wernli, A. Copetudo, D. Malz, P. Magnard, A. Akin, M. Gabureac, G. J. Norris, J. I. Cirac, A. Wallraff, and C. Eichler, *Nat. Commun.* **11**, 4877 (2020).
- [17] M. Pompili, S. L. N. Hermans, S. Baier, H. K. C. Beukers, P. C. Humphreys, R. N. Schouten, R. F. L. Vermeulen, M. J. Tiggelman, L. dos Santos Martins, B. Dirkse, S. Wehner, and R. Hanson, *Science* **372**, 259 (2021).
- [18] A. Ruskuc, C.-J. Wu, E. Green, S. L. N. Hermans, W. Pajak, J. Choi, and A. Faraon, *Nature (London)* **639**, 54 (2025).
- [19] J. Shi, S. Zhang, Y. Wu, Y. Sun, Y. Liang, H. Wang, Y. Pu, and L. Duan, *Phys. Rev. Lett.* **135**, 150802 (2025).
- [20] M. Canteri, J. Bate, I. Mishra, N. Friis, V. Krutyanskiy, and B. P. Lanyon, *arXiv:2510.15693*.
- [21] R. A. Bertlmann and N. Friis, *Modern Quantum Theory—From Quantum Mechanics to Entanglement and Quantum Information* (Oxford University Press, Oxford, United Kingdom, 2023).
- [22] G. Tóth, *Phys. Rev. A* **85**, 022322 (2012).
- [23] R. Raussendorf and H. J. Briegel, *Phys. Rev. Lett.* **86**, 5188 (2001).
- [24] H. J. Briegel and R. Raussendorf, *Phys. Rev. Lett.* **86**, 910 (2001).
- [25] A. J. Scott, *Phys. Rev. A* **69**, 052330 (2004).
- [26] M. Epping, H. Kampermann, C. Macchiavello, and D. Bruß, *New J. Phys.* **19**, 093012 (2017).

- [27] M. Pivoluska, M. Huber, and M. Malik, *Phys. Rev. A* **97**, 032312 (2018).
- [28] J. Ribeiro, G. Murta, and S. Wehner, *Phys. Rev. A* **97**, 022307 (2018).
- [29] S. Bäuml and K. Azuma, *Quantum Sci. Technol.* **2**, 024004 (2017).
- [30] H. Yamasaki, A. Pirker, M. Murao, W. Dür, and B. Kraus, *Phys. Rev. A* **98**, 052313 (2018).
- [31] M. Huber and M. Plesch, *Phys. Rev. A* **83**, 062321 (2011).
- [32] H. Yamasaki, S. Morelli, M. Miethlinger, J. Bavaresco, N. Friis, and M. Huber, *Quantum* **6**, 695 (2022).
- [33] C. Palazuelos and J. I. de Vicente, *Quantum* **6**, 735 (2022).
- [34] K. Baksová, O. Leskovjanová, L. Mišta, Jr., E. Agudelo, and N. Friis, *Quantum* **9**, 1699 (2025).
- [35] L. T. Weinbrenner, K. Baksová, S. Denker, S. Morelli, X.-D. Yu, N. Friis, and O. Gühne, [arXiv:2412.18331](https://arxiv.org/abs/2412.18331).
- [36] Y.-A. Chen, R. Zhang, Y.-Y. Fei, Z. Liu, X. Zhang, X.-F. Yin, Y. Mao, L. Li, N.-L. Liu, X. Ma, and J.-W. Pan, Entanglement Activation in Multiphoton Distillation Networks (2024), [10.21203/rs.3.rs-3828402/v1](https://arxiv.org/abs/10.21203/rs.3.rs-3828402/v1).
- [37] J. T. Barreiro, P. Schindler, O. Gühne, T. Monz, M. Chwalla, C. F. Roos, M. Hennrich, and R. Blatt, *Nat. Phys.* **6**, 943 (2010).
- [38] M. Hofmann, A. Osterloh, and O. Gühne, *Phys. Rev. B* **89**, 134101 (2014).
- [39] B. Jungnitsch, T. Moroder, and O. Gühne, *Phys. Rev. Lett.* **106**, 190502 (2011).
- [40] A. Peres, *Phys. Rev. Lett.* **77**, 1413 (1996).
- [41] P. Horodecki, *Phys. Lett. A* **232**, 333 (1997).
- [42] See Supplemental Material at <http://link.aps.org/supplemental/10.1103/kv4s-tfc6> for details on the two-copy GME witness, algorithm for proving biseparability, and uncertainty calculation of a witness mean value.
- [43] M. Ringbauer, M. Meth, L. Postler, R. Stricker, R. Blatt, P. Schindler, and T. Monz, *Nat. Phys.* **18**, 1053 (2022).
- [44] A. Sørensen and K. Mølmer, *Phys. Rev. Lett.* **82**, 1971 (1999).
- [45] Z. Hradil, J. Řeháček, J. Fiurášek, and M. Ježek, Maximum-likelihood methods in quantum mechanics, in *Quantum State Estimation*, edited by M. Paris and J. Řeháček (Springer, Berlin, Heidelberg, 2004), pp. 59–112.
- [46] R. Stárek, T. Gollerthan, O. Leskovjanová, M. Meth, P. Tirlir, N. Friis, M. Ringbauer, and L. Mišta, Jr., Experimental verification of multi-copy activation of genuine multipartite entanglement—data and code, [10.5281/zenodo.17357727](https://arxiv.org/abs/10.5281/zenodo.17357727) (2025).